Arch. Mech., **51**, 6, pp. 785–803, Warszawa, 1999

Shape memory alloy preparation for multiaxial tests and identification of fundamental alloy performance

K. TANAKA ([1]), K. KITAMURA ([2]) and S. MIYAZAKI ([2])

([1]) *Department of Aerospace Engineering*
Tokyo Metropolitan Institute of Technology
J-191-0065 Hino/Tokyo, Japan
e-mail: kikitana@astan1.tmit.ac.jp

([2]) *Institute of Materials Science*
University of Tsukuba
J-305-8573 Tsukuba, Japan
e-mail: miyazaki@mat.ims.tsukuba.ac.jp

TiNi SHAPE MEMORY alloy preparation for the multiaxial tests was explained. Stable response of the alloy was realized, not by training but by an effective combination of the alloying technique and the heat treatment: Ti-51.0at%Ni polycrystalline shape memory alloy heat-treated by annealing at 673 K for 3.6 ks followed by cooling in a furnace. Some preliminary tests were performed to identify the fundamental alloy characteristics: the transformation temperatures, the stress-strain curves at several temperatures and the strain-temperature curves under constant hold stresses.

Keywords: TiNi shape memory alloy, Multiaxial tests, Alloying and heat treatment, Ni-rich shape memory alloy, Training.

1. Introduction

IN RECENT APPLICATIONS of shape memory alloys (SMAs), SMA devices often work under the complex multiaxial stress states. The SMA components inside the SMA composites, for example, are actually subjected to such conditions, although the composites themselves might be operated under a simple load when performing their special function associated with the shape memory effect [1, 2]. Of course, larger size SMA devices, such as pipe fasteners, have to carry the complex mechanical loads, in addition to thermal load [3, 4].

In order to design effectively such SMA devices, one has to know as exactly as possible the thermomechanical response of SMA under multiaxial stress states. Only a few studies have been carried out so far on the thermomechanical behavior of SMAs under the multiaxial stress states; SITTNER and TOKUDA [5 – 7] and ROGUEDA *et al.* [8] in Cu-based SMA, NISHIMURA *et al.* [9 – 11] in Fe-based

SMA and SEHITOGLU *et al.* [12, 13] in TiNi and Cu-based SMAs. Torsion-tension (compression) tests were preferably carried out with thin-walled tubular specimens. The martensitic and reverse transformation start/finish conditions and the stress-strain-temperature curve hysteresis were intensively investigated. Asymmetry of the stress-strain in tension and compression [14, 15], and of the martensitic transformation start condition in the stress-temperature space were clearly observed in all SMAs, thus approving the theory with the third invariant of the stress tensor [16, 17]. The normality law was also investigated with a strong expectation that the transformation condition, represented by a surface in the stress-temperature space, could play a role of a potential, just like in plasticity, leading to the evolution equations for the internal variables, such as the transformation strain and the volume fraction of martensite [18]. The accumulation of the data is, however, still necessary to establish a rational theoretical framework in transformation thermomechanics of SMAs.

The SMA sample for the multiaxial tests has to exhibit always a stable response to repeated thermomechanical loads, since a single specimen is usually used repeatedly in the test. In order to realize a stable performance, SMAs are often "trained" prior to actual operations [19, 20]. This kind of stabilization of the alloy properties should not be employed when investigating the intrinsic alloy characteristics, since the subsequent alloy performance is strongly influenced by the directional training. Alloying technique and the heat treatment, studied intensively by MIYAZAKI *et al.* [19, 20], should be the strategy to achieve the requirement.

In 1996 the Japanese-Polish cooperative study "Testing and Modelling the Behavior of Shape Memory Alloys" has started through the Japan-Europe Research Cooperative Program promoted by both the Japan Society of Promotion of Sciences and the Polish Academy of Sciences. The torsion-tension (compression) tests with the thin-walled tubular specimen in TiNi shape memory alloy were performed to investigate the thermomechanical behavior associated with the reorientation of the R-phase or the martensite variants, and with the stress-induced R-phase or martensitic transformation [21 – 24]. In this paper, the method of alloy preparation for the Project is explained, and some preliminary alloy properties are determined.

2. Alloy strategy for multiaxial tests

2.1. Requirements for multiaxial tests

Following points should be carefully taken into account when preparing the alloy for the multiaxial tests in SMAs: First of all, as in the case of plasticity, the size of the specimen should be large enough to realize a uniform stress and

strain state inside the specimen. The experimental system, used in the present Japanese-Polish cooperative project, actually requires the dimensions of the thin-walled tubular specimen to be the following: 20 mm in outer diameter, 1.5 mm in wall thickness, 50 mm in parallel part, 120 mm in total length and 26 mm in the maximum diameter for the grip ends [25] (cf. Fig. 1). One should note that the size is extremely large compared to the specimens employed in the usual tests in SMAs. Needless to say, the alloy properties should be isotropic.

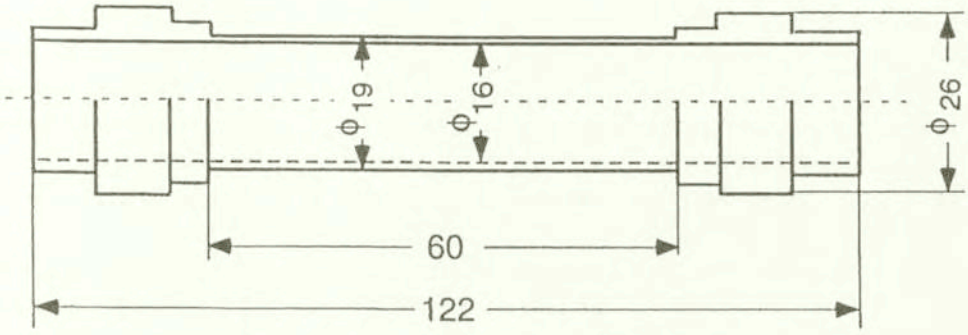

FIG. 1. Test specimen for multiaxial tests.

Secondly, almost perfect stability of the thermomechanical alloy properties is required since the specimen must be used repeatedly in the tests. The irreversible change of internal structure on the microscopic level should appear in the specimen during the tests. This requirement strongly limits the method of stabilizing the alloy response. The strain-temperature or the stress-strain hysteresis loop usually changes cycle by cycle during thermal or mechanical cyclic loading, and the loop gradually tends to a limit loop, after some 50 to 100 cycles of loading [19, 20]. The dislocations and other lattice defects are introduced during cycling, which increase the critical stress for slip, resulting in a stable response of the alloy. This way of stabilizing the alloy performance, the training, cannot be employed in the present alloy preparation since the direction of stressing strongly influences the subsequent alloy response, although a stable performance is finally observed. The alloy response after training cannot be regarded as the intrinsic characteristics of the alloy. Not the training, but the alloying technique and the appropriate heat treatment should, therefore, be the method to achieve a stable response of the alloy.

2.2. Alloying strategy to acquire stable response

According to a comprehensive investigation by MIYAZAKI *et al.* [19, 20], the critical stress for slip is highly sensitive in TiNi SMAs to both the thermomechanical treatment and the Ni content. They have clearly demonstrated that two

strategies effectively work in order to raise the critical stress for slip, and as a result, to stabilize, during cycling, the transformation temperatures of both the R-phase and martensitic transformation. Introduction of fine precipitates, actually Ti_3Ni_4 precipitates, and the introduction of dislocations. The precipitation hardening and the hardening due to a high dislocation density are the physical mechanisms behind the phenomenon.

The Ti_3Ni_4 precipitates, of the order of 40 nm in size, were found to form uniformly with an optimal state for both their size and density when the alloy specimen was aged at 673 K for 3.6 ks. However, the specimens for the multiaxial stress tests demand considerably large bar sizes, i.e., larger than 26 mm in diameter, as raw materials. It is not expected to introduce uniform plastic strain throughout the whole rod of such dimension. For this reason, the dislocation hardening mechanism was not applied for the present investigation. In order to use the precipitation hardening mechanisms, a Ni-rich Ti-51.0at% Ni polycrystalline alloys was selected for the multiaxial stress tests.

The Ti-51.0at% Ni alloy ingot was made in a carbon crucible by high-frequency vacuum induction melting. The ingot was hot forged at the temperature range between 1073 K and 1173 K to make bars of 28 mm in diameter and 150 mm in length. The bars were machined to make the outer shape and spark-cut to make the inner shape of the thin-walled turbular specimens for the multiaxial stress tests. Smaller bars of about 15 mm in diameter were extracted by spark-cutting. Rectangular tensile specimens, 1.0 mm in thickness, 2.0 mm in width, 50 mm in length and 30 mm in gauge length, were made from small bars. The specimens for both multiaxial stress tests and tensile tests were etched by acid solution after mechanical polishing. They were annealed at 673 K for 3.6 ks followed by cooling in a furnace. They were again chemically polished to remove slightly oxidized surface layers. The average grain size was about 30 μm.

The experimental results in the torsion-tension (compression) tests with this specimen are reported elsewhere [25]. A stable response of the alloy is actually demonstrated there, and the isotropy of the alloy characteristics is discussed as an important issue.

3. Fundamental alloy performance

Fundamental uniaxial alloy performance was identified for designing an effective experimental program under the multiaxial stress state.

3.1. Transformation temperatures

Transformation temperatures were determined by means of DSC (differential scanning calorimetry) tests. In Fig. 2, the upper curves were measured by

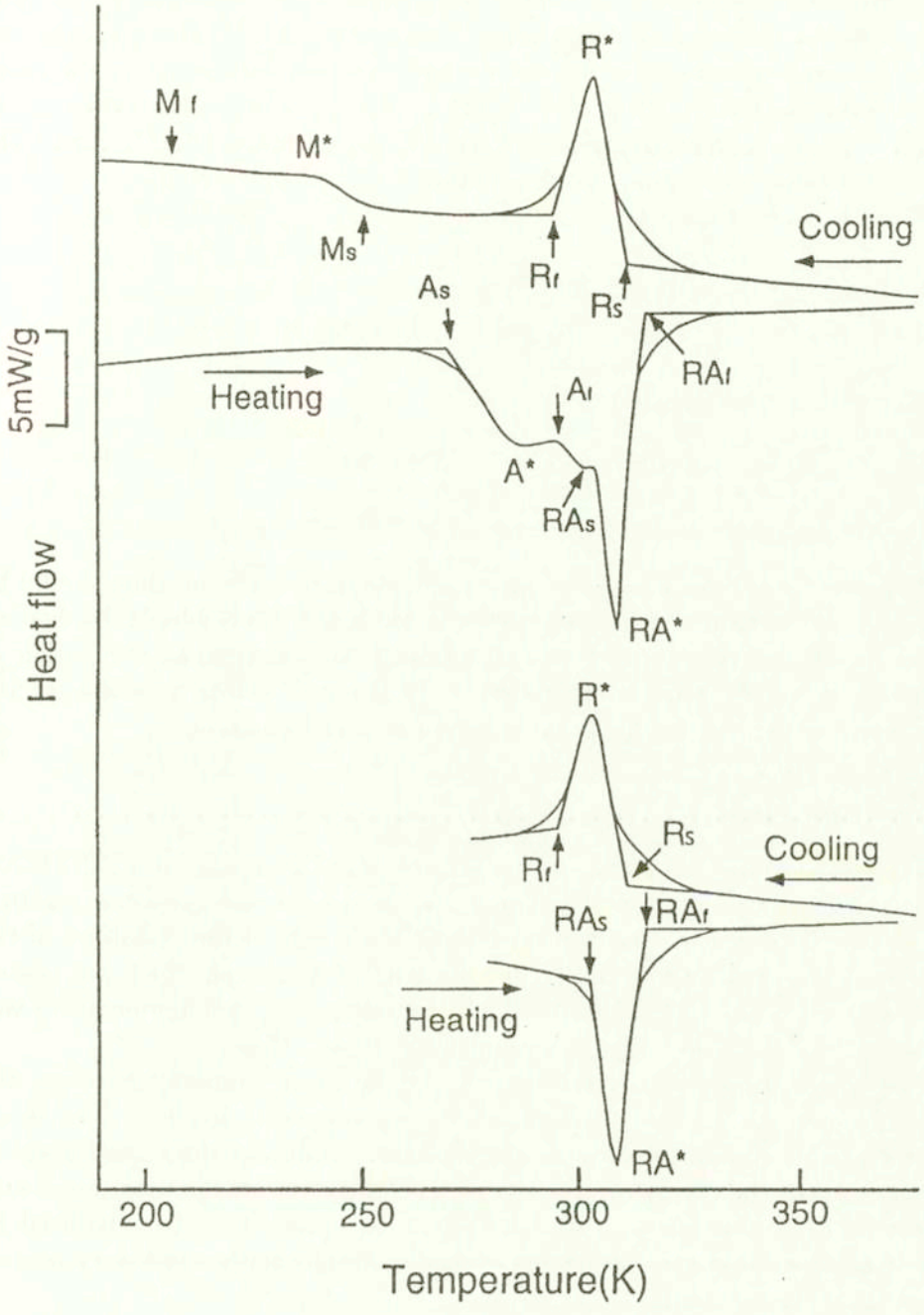

FIG. 2. DSC tests and transformation temperatures.

varying temperature between 150 K and 380 K in order to observe tqo peaks associated with the R-phase and martensitic transformations. The curve upon cooling reveals the two transformations to be well separated. However, the two peaks for the reverse transformations partially overlap each other in the curve upon heating. Therefore, a partial thermal cycling test was also conducted to observe only the R-phase transformation as shown by the lower DSC curves. The results of the transformation temperatures are summarized as follows:

R-phase transformation:

$$\text{Rs} = 306\ \text{K}, \qquad \text{Rf} = 293\ \text{K},$$

$$\text{RAs} = 305\ \text{K}, \qquad \text{RAf} = 316\ \text{K}.$$

Martensitic transformation:

$$\text{Ms} = 253\ \text{K}, \qquad \text{Mf} = 208\ \text{K},$$

$$\text{As} = 268\ \text{K}, \qquad \text{Af} = 306\ \text{K}.$$

The result indicates that the multiaxial tests in the present alloy should be carried out at the temperature range between 200 K and 375 K when investigating all the aspects of transformation and deformation behavior, as a function of temperature, including the reorientation of the R-phase and martensite variants, and the stress-induced R-phase and martensitic transformations.

3.2. Stress-strain curves

The isothermal stress-strain curves were obtained by means of a INSTRON-type testing machine at several temperatures in the proposed test temperature range. The displacement was measured from the stroke of the crosshead of the machine. The specimen was dipped in a hot bath of silicon oil, which was heated by an electric heater or cooloed by liquid nitrogen. The test temperature was controlled by ± 0.5 K in both the specimen length and time.

The results are summarized in Fig. 3. At the lower temperature range, the thermally induced R-phase variants are reoriented during loading. The reorientation of the martensite variants then follows, exhibiting the second stage of deformation on the stress-strain curves. The pseudoelasticity associated with the martensitic transformaton is observed above 300 K. The stress-induced R-phase transformation precedes the martensitic transformation in a very narrow temperature range around 336 K.

This characteristic is clearly confirmed when the critical stresses necessary to start the reorientation or transformation are plotted in Fig. 4, where σ_{M}, σ_{A} and σ_{R} stand for the martensite start stress, austenite start stress and the

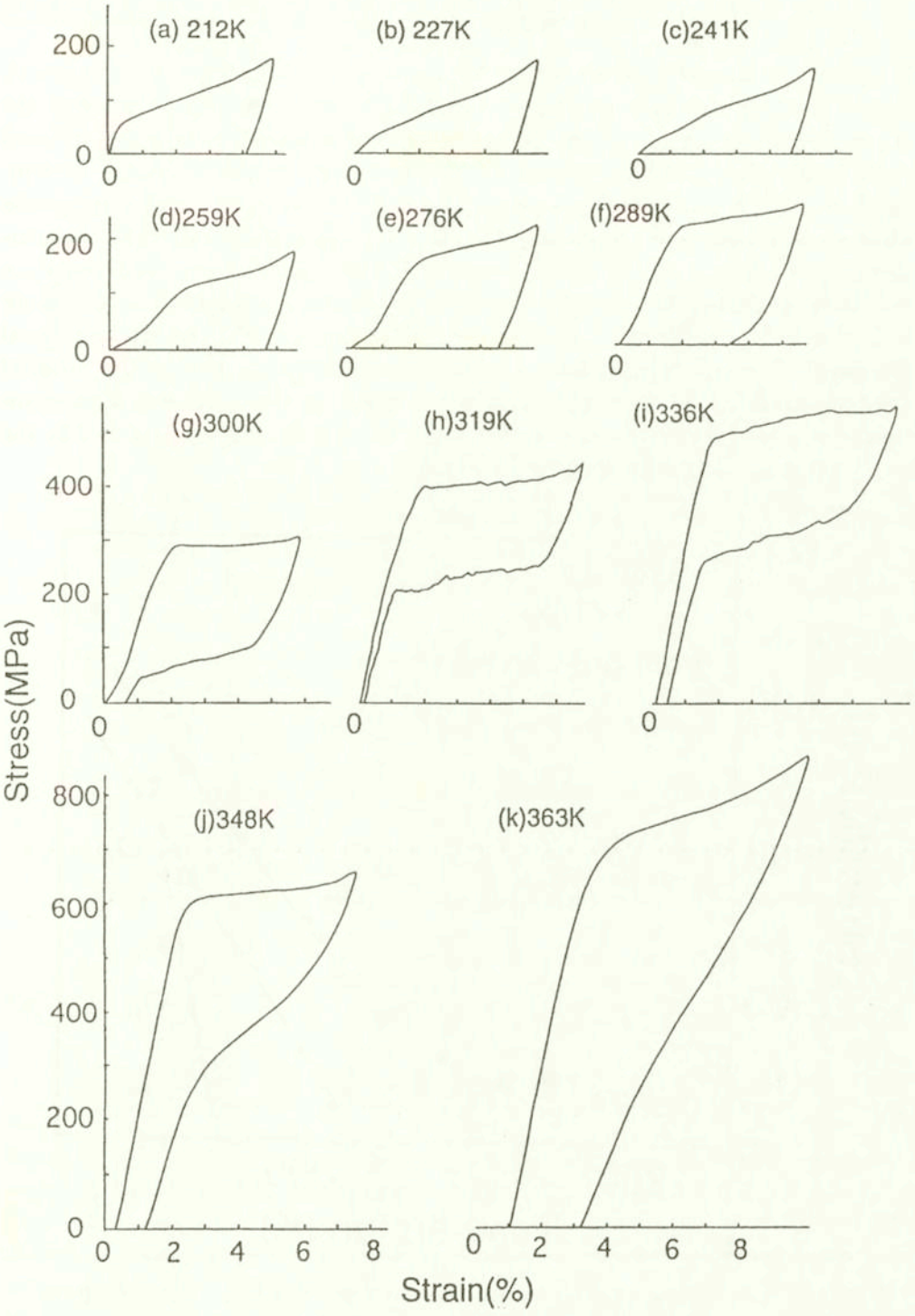

FIG. 3. Isothermal stress-strain curves.

R-phase transformation start stress, respectively (See Fig. 5 for the definition). The critical stresses need for the reorientation of the martensite variants or the R-phase variants are low compared to the critical stresses for the stress-induced transformations. The former critical stresses are nearly insensitive to the temperature. The linear temperature-dependence indicated by the lines corresponds to the Clausis-Clapeyron relation [21 – 23]. The result suggests that the multiaxial tests should start from the study of R-phase reorientation process, since the tests can safely be carried out at the lower stress level than in the other processes: the reorientation of the martensite variants, and the stress-induced R-phase and martensitic transformations. Phase diagram, not on the uniaxial stress-temperature plane like the one in Fig. 4 but, in the multiaxial stress-temperature space, should be one of the issues to be specially investigated in the study programs following the present paper.

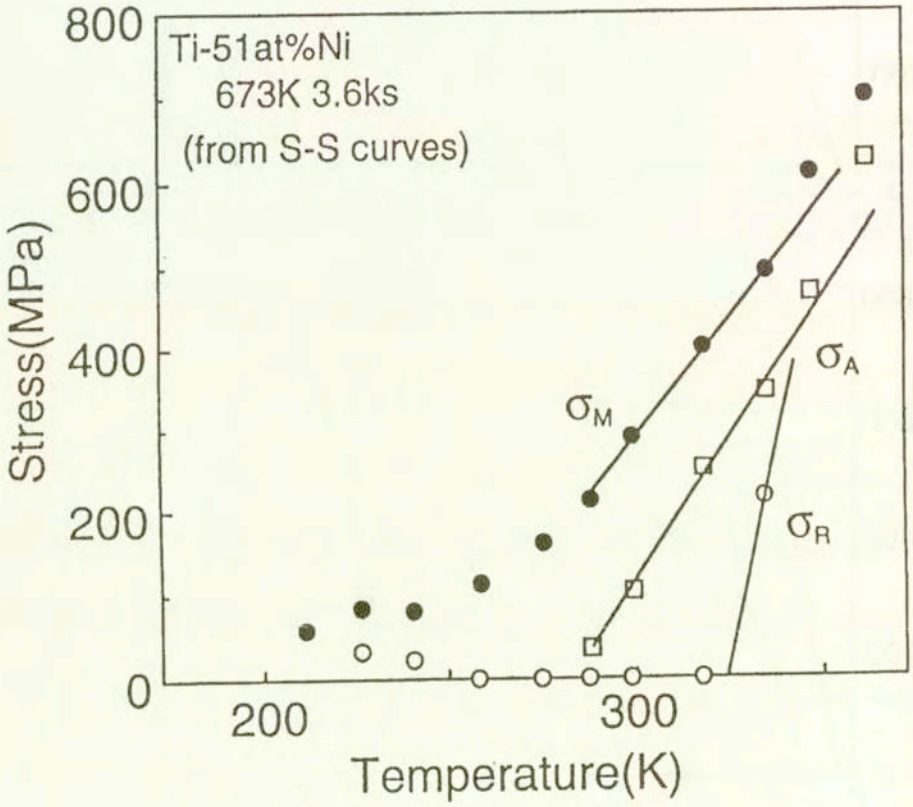

FIG. 4. Critical stress to start reorientation or transformations; Phase diagram.

Figure 5 illustrated the stress and strain characteristic parameters which identify the stress-strain curve at typical temperature ranges.

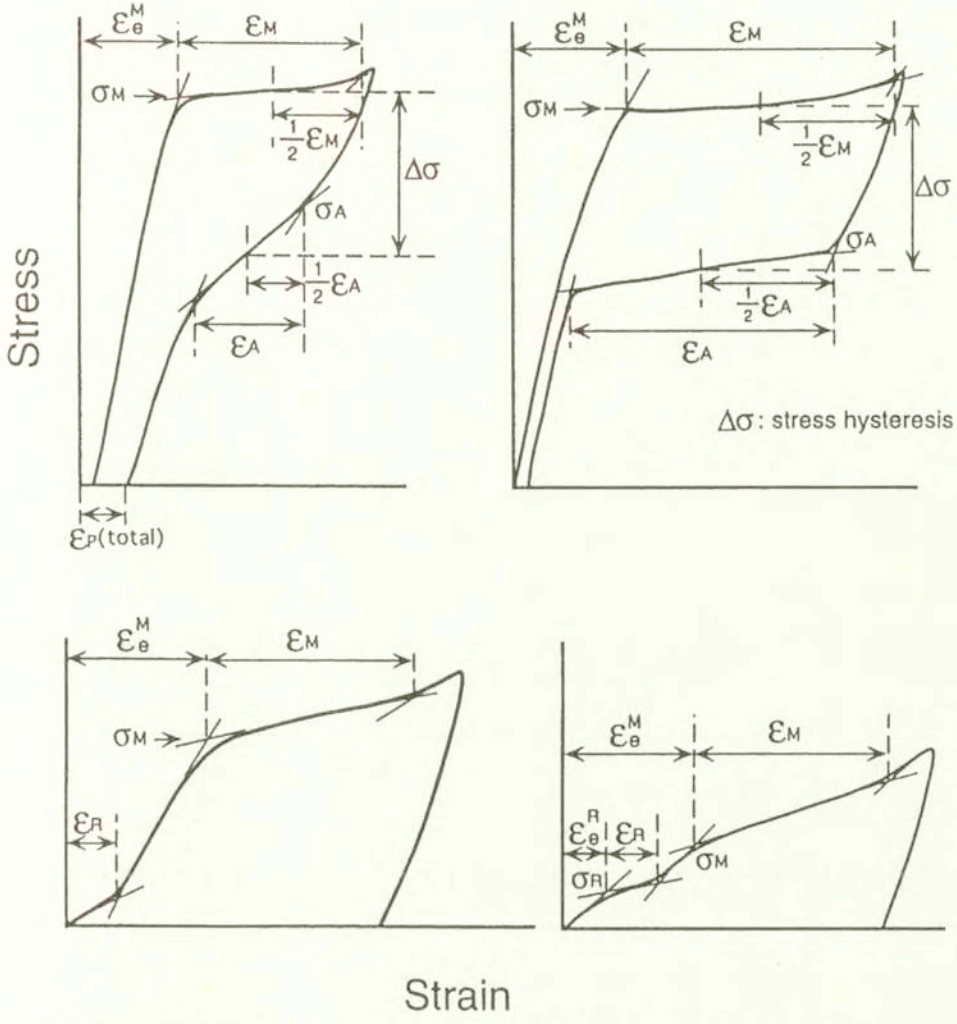

FIG. 5. Schematic diagrams of stress-strain curves, defining the characteristic stress and strain parameters.

The evolution of the strain parameters are plotted in Figs. 6 and 7. The martensitic transformation strain ε_M and the reverse transformation strain ε_A, having the values of 3 to 5%, increase with the martensite start stress σ_M, meaning they strongly depend on the temperature. As σ_M becomes larger, i.e., at higher temperature range, a full shape recovery is not expected after a full martensitic transformation. The R-phase transformation strain ε_R, which is almost temperature-independent, is much smaller in the whole temperature range than the martensitic transformation strain ε_M. It should be noted that the strain components, ε_e^R and ε_e^M, do not stand for the elastic component in a strict sense, but represent roughly the reversible part of the total strain.

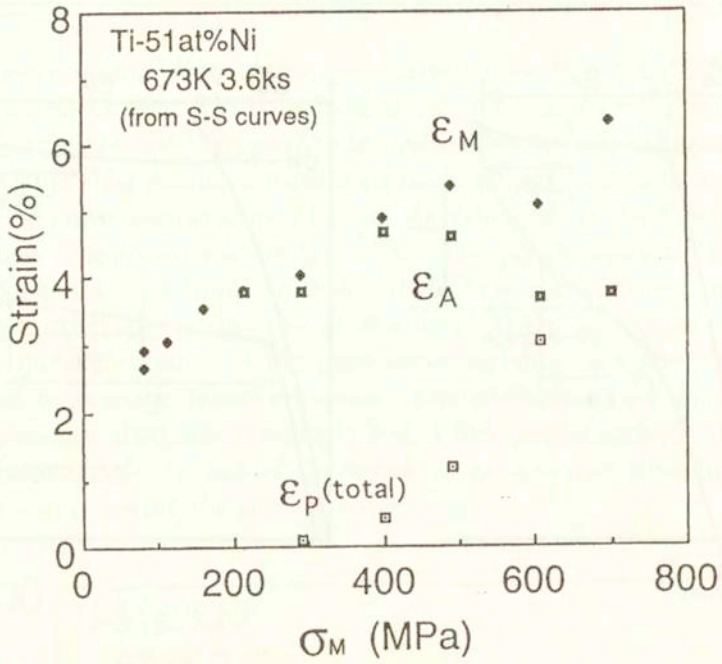

FIG. 6. Transformation strains in martensitic and reverse transformation, and evolution of irreversible strain.

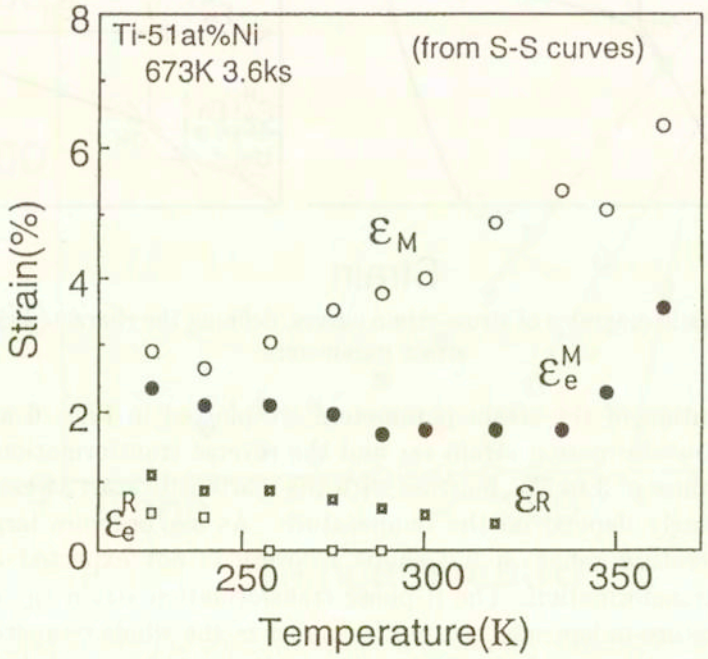

FIG. 7. Transformation strains in martensitic and R-phase transformations.

The stress hysteresis $\Delta\sigma$, which is defined in Fig. 5 and measures the size of the hysteresis loop at the pseudoelastic temperature range, depends on the temperature as plotted in Fig. 8. At the pseudoelastic temperature range around 320 K, where the full shape recovery is observed, the stress hysteresis exhibits the minimum value.

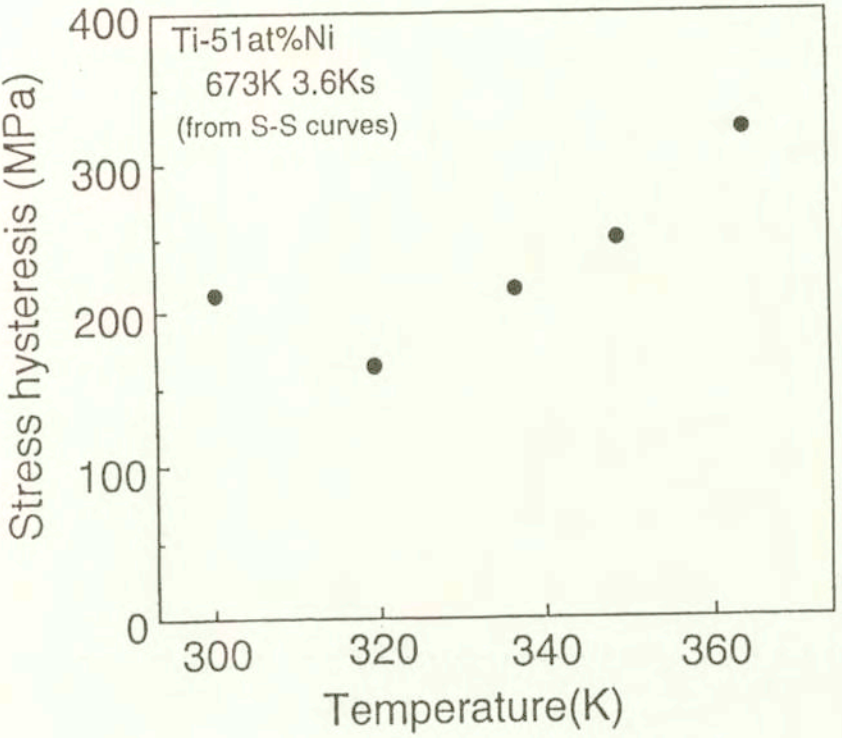

FIG. 8. Temperature-dependence of stress hysteresis.

The stress hysteresis normally decreases with increasing temperature or stress. However, it increases when considerable amount of plastic strain is induced during transformation as shown by the data at higher temperatures. This suggests that all the necessary tests associated with the martensitic transformation must be conducted at the temperature range below 320 K.

3.3. Strain-temperature curves under constant stress

Strain-temperature curves were determined under constant hold stresses with the same experimental system explained in Sec. 3.2. The cooling and heating rates were about 4 K/min in the whole tests. The result is summarized in Figs. 9 and 10. Figure 9 shows the shape memory behavior associates with both the

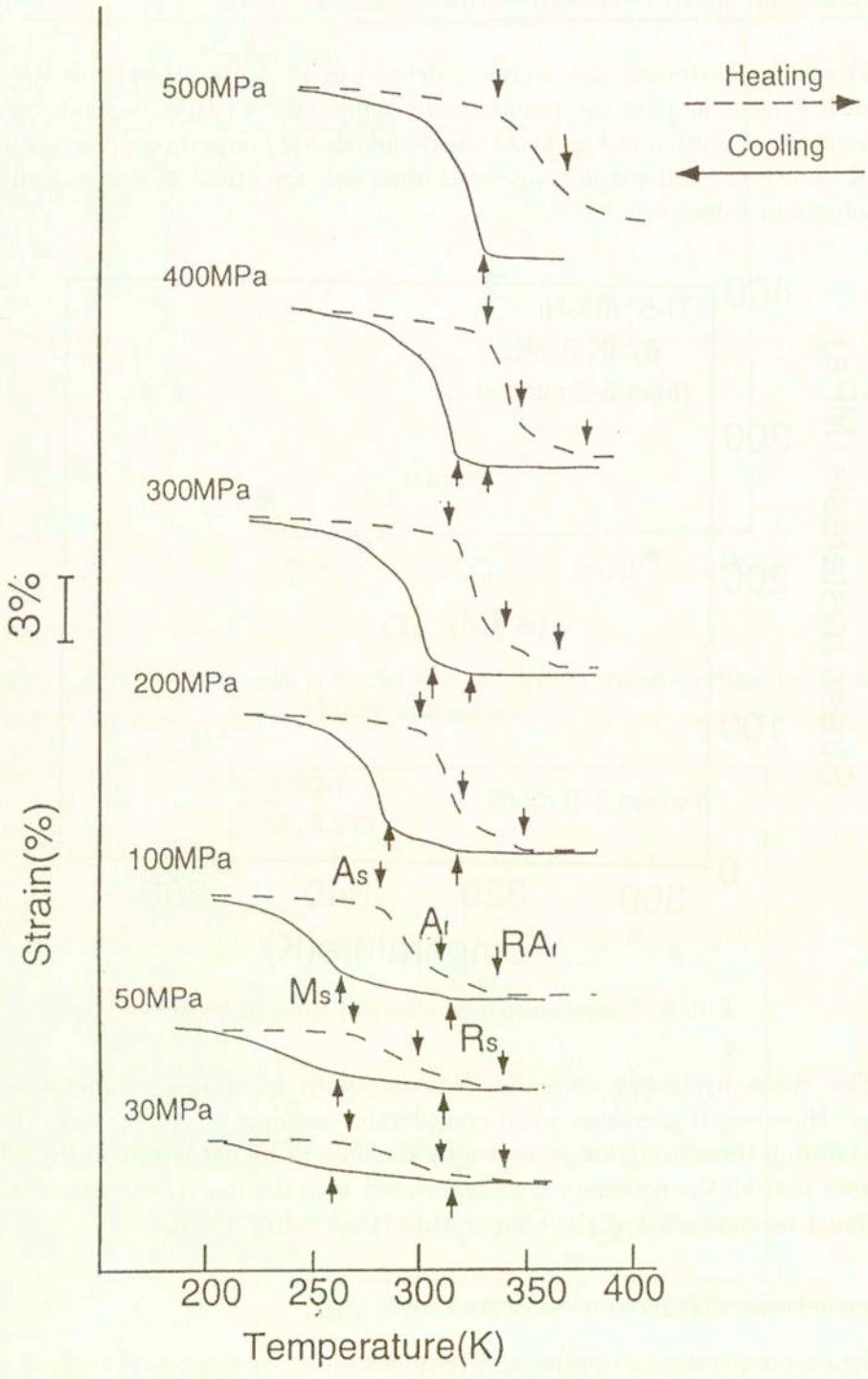

FIG. 9. Strain-temperature curves under constant hold stress.

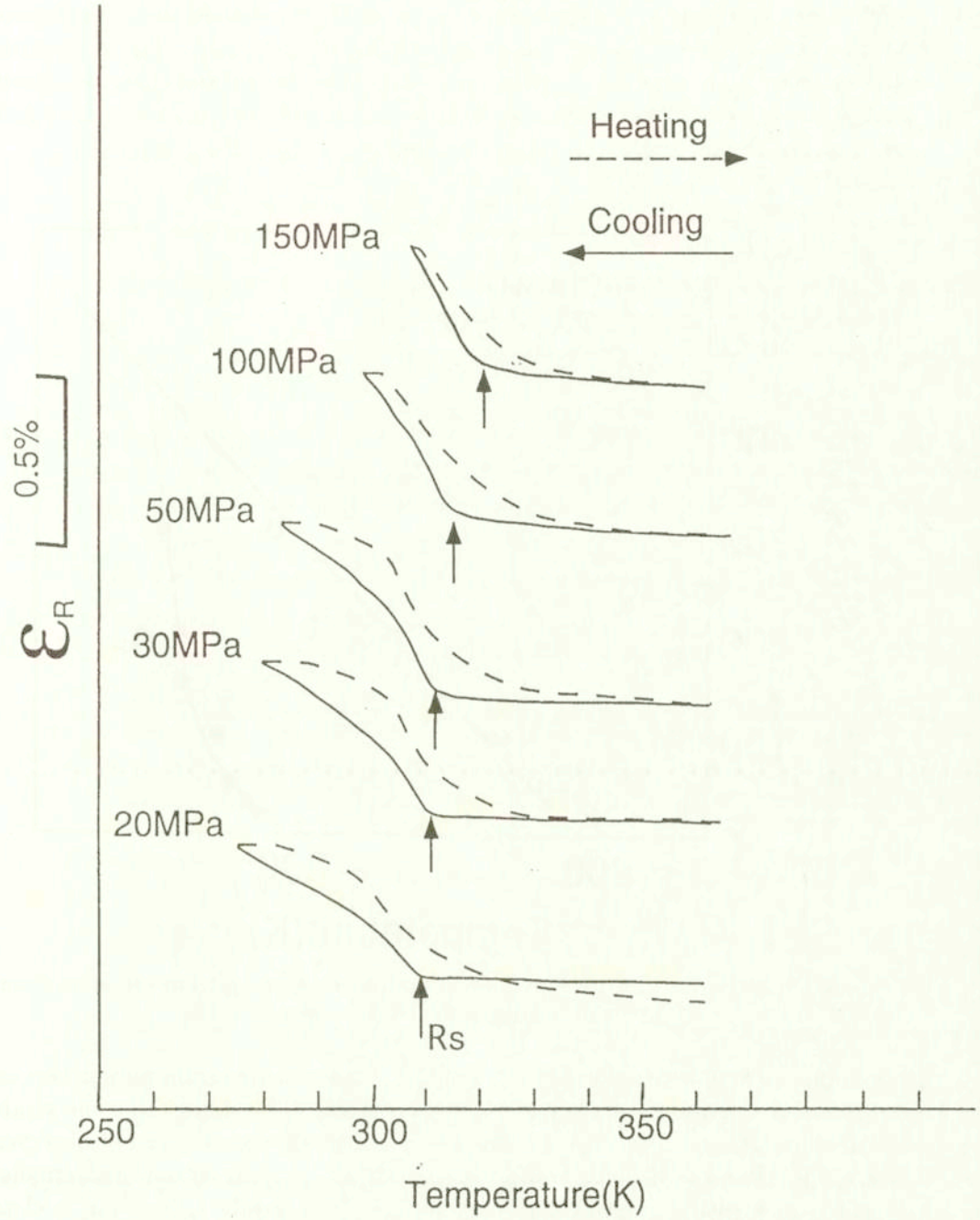

FIG. 10. Strain-temperature curves under constant hold stress; Details at lower hold stress level.

R-phase and martensitic transformations, while Fig. 10 shows that associated with only the R-phase transformation. The solid and dashed lines correspond to the shape changes upon cooling and heating, respectively. The hold-stress dependence of the transformation temperatures, Ms, As, Rs and RAf, are clearly observed. One can now construct another phase diagram shown in Fig. 11, which reveals clearer characteristics of the transformation stresses σ_M and σ_R.

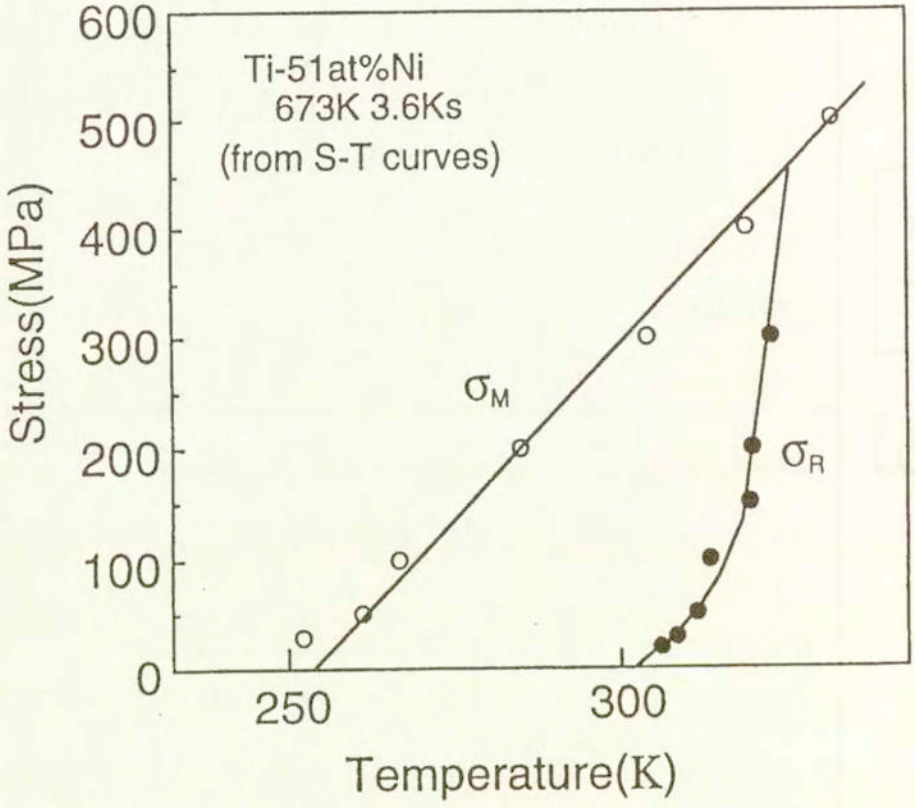

FIG. 11. Critical stress to stress-induced martensitic and R-phase transformation determined from strain-temperature curves.

Figure 12 represents the definition of the characteristic strain parameters on the strain-temperature curves under constant stress. The change in some strain parameters are shown in Figs. 13 and 14. A full shape recovery is not observed above 300 MPa. The R-phase transformation strain ε_R, is about ten times smaller than the martensitic transformation strain ε_M. It is exhibits, however, a clear sensitivity to the hold stress. This a point to be effectivelly used in practical applications.

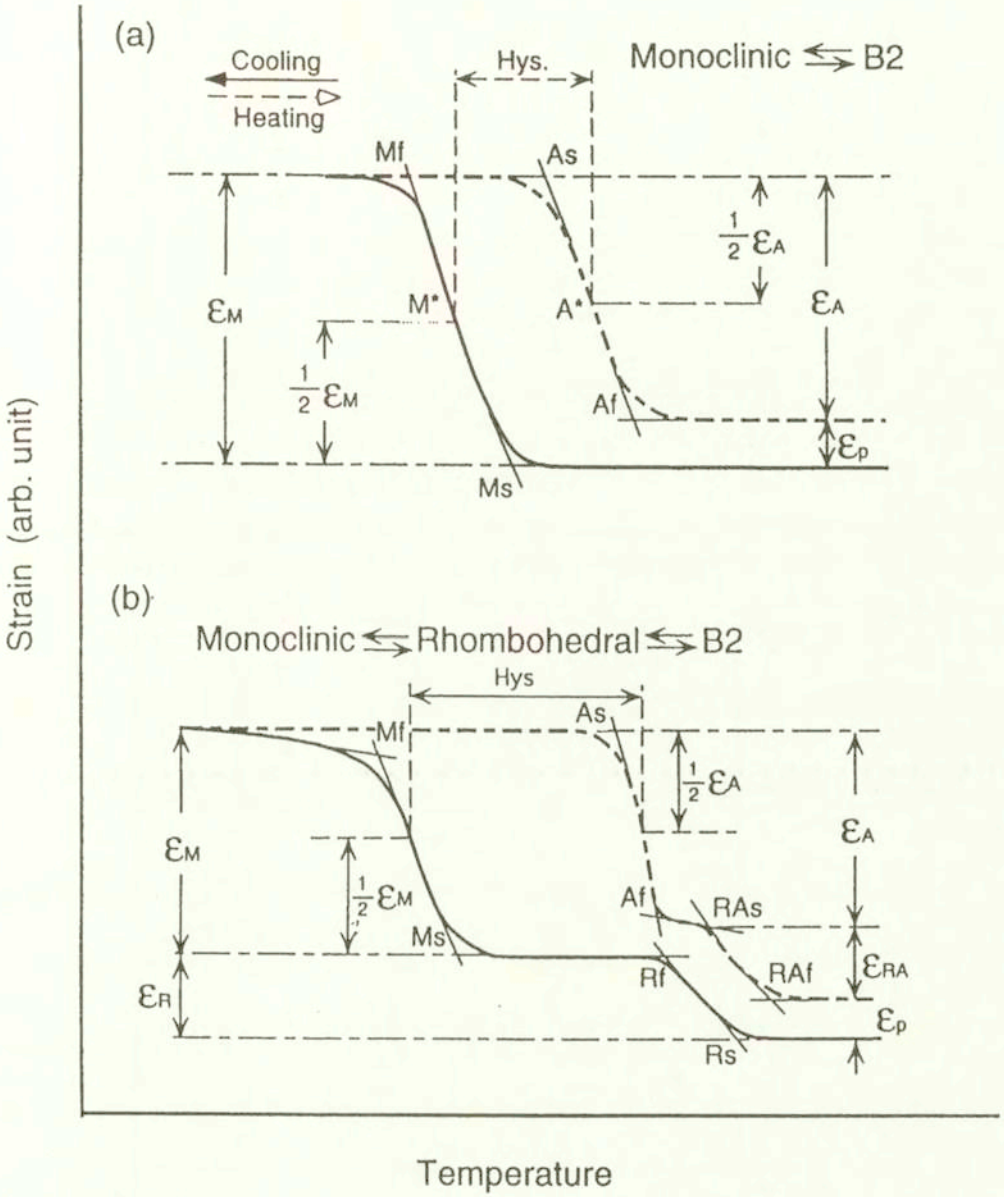

FIG. 12. Schematic diagrams of strain-temperature curves under hold stress, defining the characteristic strain parameters and transformation temperatures; (a) single stage transformation associated with the typical transformation from B2 to M(monoclinic), and (b) two-stage transformation from B2 to E(rhombohedral) to M.

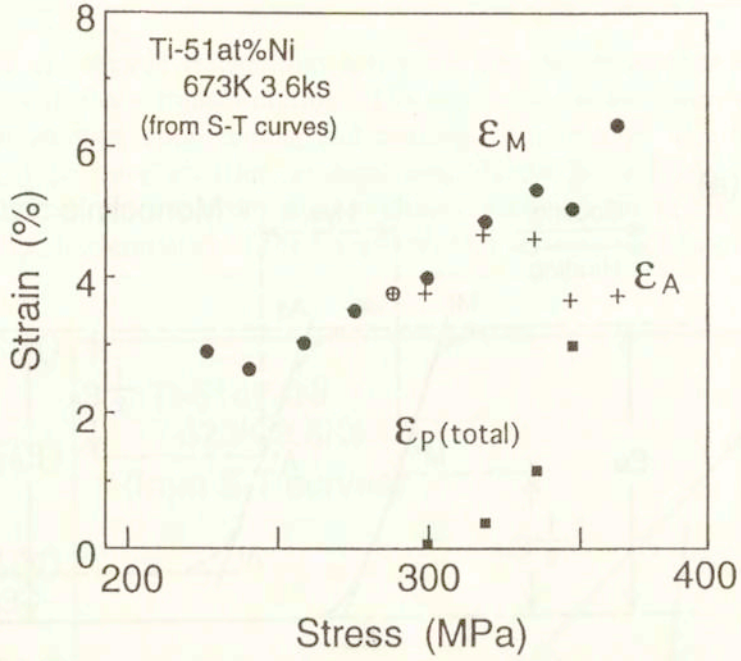

FIG. 13. Transformation strain in martensitic and reverse transformations, and evolution of irreversible strain determined from strain-temperature curves.

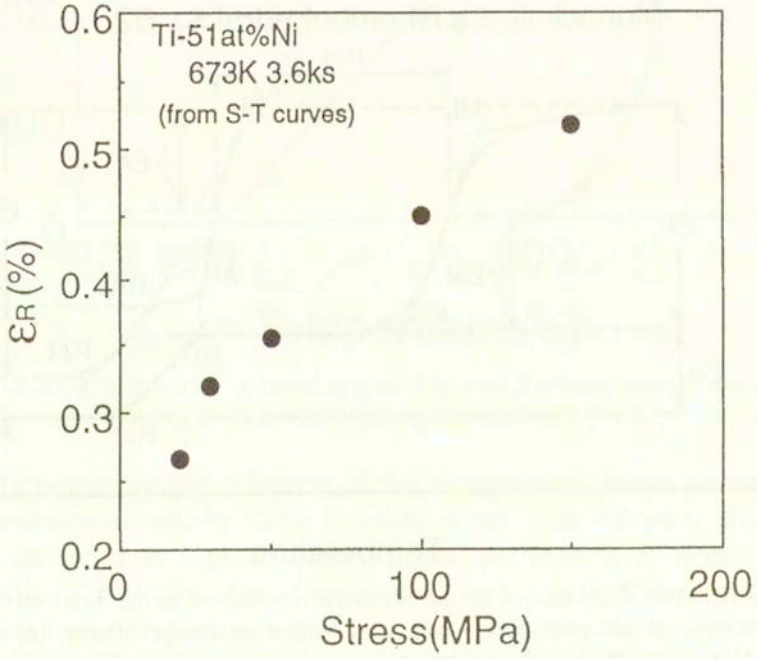

FIG. 14. Evolution of R-phase transformation strain.

The temperature hysteresis, plotted in Fig. 15, shows again that the loop is closed at the stress range around 300 MPa.

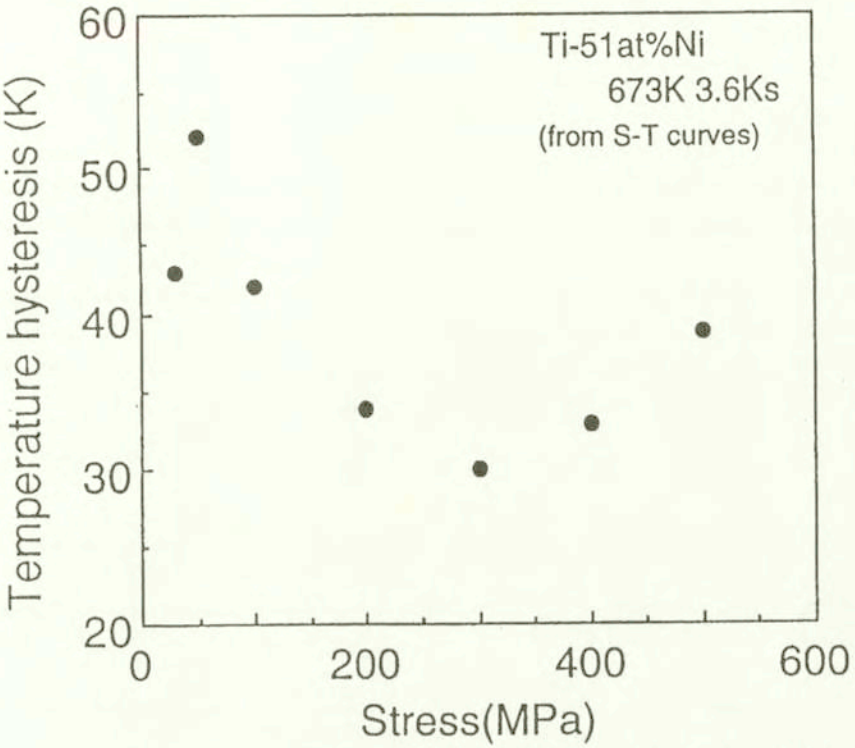

FIG. 15. Stress-dependence of temperature hysteresis.

4. Concluding remarks

A Ti-Ni shape memory alloy sample was prepared for the multiaxial tests. The training was not employed to achieve a stable response of the alloy since the method of training, more directly, the direction of stressing, strongly influences the subsequent alloy performance, thus eliminating totally the intrinsic property of the alloy.

Effective combination of the alloying technique and the heat treatment, Ti-51.0at%Ni polycrystalline shape memory alloy heat-treated by annealing at 673 K for 3.6 ks followed by cooling in a furnace, enables us to machine the thin-walled tubular specimens, 19 mm in outer diameter, 1.5 mm in wall thickness, 26 mm in maximum diameter and 122 mm in length.

Some preliminary tests were performed to identifity the fundamental alloy characteristics; the transformation temperatures, the stress-strain curves

at several temperatures and the strain-temperature curves under constant hold stresses. The data were used to design an effective experimental program.

The multiaxial tests with this test piece actually revealed that the alloy is prepared perfectly, without showing any macroscopic shape irreversibility during a series of tests [25].

Acknowledgments

The authors are grateful for supply of the alloy by Mr. T. UEKI and for preparation of the specimens by Messrs. M. TAIRA, M. KADOWAKI and H. KIKUCHI.

One of the authors (K.T.) expresses his thanks for the financial support by the Special Research Fund Tokyo Metropolitan Government. The financial aid provided by the Japan Society of Promotion of Sciences through the Japan-Europe Research Cooperative Program is also acknowledged.

References

1. E.P. GEORGE, R. GOTTHARDT, K. OTSUKA, S. TROLIER-MCKINSTRY and M. WUN-FOGLE [Eds.], *Materials for smart systems* II, Materials Research Society, Pittsburgh, 1997.
2. Z.G. WEI, R. SANDSTRÖM and S. MIYAZAKI, *Shape-memory materials and hybrid composites for smart systems, Part* I *and* II, J. Materials Sci., **33**, 3743–3762, 3763–3783, 1998.
3. T.W. DUERIG, K.M. MELTON, D. STÖCKEL and C.M. WAYMAN, *Engineering aspects of shape memory alloys*, Butterworth-Heinemann, London 1990.
4. Y. MORIYA, H. KIMURA, S. ISHIZAKI, S. HASHIZUME, S. SUZUKI, H. SUZUKI and T.SAMPEI, *Properties of* Fe-Cr-Ni-Mn-Si(-Co) *shape memory alloys*, J. Phys. IV, **1**, 4, 433–438, 1991.
5. M. TOKUDA, P. SITTNER, M. TAKAKURA and YE MEN, *Experimental study on performances in* Cu-*based shape memory alloy under multiaxial loading conditions*, Materials Sci. Research Int., **1**, 260–265, 1995.
6. P. SITTNER and M. TOKUDA, *Reorientation in combined stress-induced martensite?*, J. Phys., **8**, 5, 1003-1008, 1995.
7. P. SITTNER, Y. HARA and M. TOKUDA, *Experimental study on the thermoelastic martensitic transformation in shape memory alloy polycrystal induced by combined external forces*, Metall. Mater. Trans. A, **26A**, 2923–2935, 1995.
8. C. ROGUEDA, C. LEXCELLENT and L. BOCHER, *Experimental study of pseudoelastic behaviour of a* CuZnAl *polycrystalline shape memory alloy under tension-torsion proportional and non-proportional loading tests*, Arch. Mech., **48**, 10250–1045, 1996.
9. F. NISHIMURA, N. WATANABE, T. WATANABE and K. TANAKA, *Transformation conditions in an* Fe-*based shape memory alloy under tensile-torsional loads: Martensite start surface and austenite start/finish planes*, Materials Sci. Engng. A, **264**, 232–244, 1999.
10. F. NISHIMURA, N. WATANABE and K. TANAKA, *Evolution of martensite start condition in general thermomechanical loads of an* Fe-*based shape memory alloy*, Int. J. Mech. Sci., **42**, 347–365, 1999.

11. K. TANAKA and T. WATANABE, *Transformation conditions in an* Fe*-based shape memory alloy: an experimental study*, Arch. Mech., this issue.

12. K. JACOBUS, H. SEHITOGLU and M. BLAZER, *Effect of stress state on the stress-induced martensitic transformation in polycrystalline* Ni-Ti *alloy*, Metall. Mater. Trans. A, **27A**, 1–8, 1996.

13. K. GALL, H. SEHITOGLU, H.J. MAIER and K. JACOBUS, *Stress-induced martensitic phase transformations in polycrystalline* CuZnAl *shape memory alloys under different stress states*, Metall. Mater. Trans. A, **29A**, 763–773, 1998.

14. L. ORGEAS and D. FAVIER, *Non-symmetric tension-compression behaviour of* NiTi *alloy*, J. Phys., **8**, 5, 605–610, 1995.

15. L. ORGEAS and D. FAVIER, *Stress-induced martensitic transformation of a* NiTi *alloy in isothermal shear, tension and compression*, Acta Mater., **46**, 5579–5591, 1998.

16. E. PATOOR, A. EBERHARDT and M. BERVEILLER, *Micromechanical modelling of the shape memory behavior*, [in:] L.C. BRINSON and B. MORAN [Eds.], *Mechanics of phase transformations and shape memory alloys*, AMD **189**/PVP **292**, ASME, 23–37, 1994.

17. B. RANIECKI and CH. LEXCELLENT, *Thermodynamics of isotropic pseudoelasticity in shape memory alloys*, Eur. J. Mech. A/Solids, **17**, 185–205, 1998.

18. F.D. FISCHER, E.R. OBERAIGNER, K. TANAKA and F. NISHIMURA, *Transformation-induced plasticity revised: An update formulation*, Int. J. Solids Struct., **35**, 2209–2227, 1998.

19. S. MIYAZAKI, T. IMAI, Y. IGO and K. OTSUKA, *Effect of cyclic deformation on the pseudoelasticity characteristics of* Ti-Ni *alloys*, Metall. Trans. A, **17A**, 115–120, 1986.

20. S. MIYAZAKI, *Thermal and stress cyclic effects and fatigue properties of* Ni-Ti *alloys*, [in:] T.W. DUERIG, K.N. MELTON, D. STÖCKEL and C.M. WAYMAN [Eds.], *Engineering aspects of shape memory alloys*, Butterworth-Heinemann, 394–413, London 1990.

21. S. MIYAZAKI and K. OTSUKA, *Deformation and transition behavior associated with the* R*-phase in* Ti-Ni *alloys*, Metall. Trans. A, **17A**, 53–63, 1986.

22. S. MIYAZAKI and C.M. WAYMAN, *The* R*-phase transition and associated shape memory mechanism in* TiNi *single crystals*, Acta Metall., **36**, 181–192, 1988.

23. S. MIYAZAKI, S. KIMURA and K. OTSUKA, *Shape-memory effect and pseudoelasticity associated with the* R*-phase transition in* Ti-50.5at%Ni *single crystals*, Phil. Mag. A, **57**, 467–478, 1988.

24. K. TANAKA, F. NISHIMURA, H. KATO and S. MIYAZAKI, *Transformation thermomechanics of* R*-phase in* TiNi *shape memory alloys*, Arch. Mech., **49**, 547–572, 1997.

25. B. RANIECKI, S. MIYAZAKI, K. TANAKA, L. DIETRICH and C. LEXCELLENT, *Deformation behaviour of* TiNi *shape memory alloy undergoing* R*-phase reorientation in torsion-tension (compression) tests*, Arch. Mech., this issue.

Received April 27, 1999; new version August 30, 1999.